CEAS Aeronaut J
DOI 10.1007/s13272-012-0055-7

ORIGINAL PAPER

Accurate determination of dispersion curves of guided waves in plates by applying the matrix pencil method to laser vibrometer measurement data

F. Schöpfer · F. Binder · A. Wöstehoff · T. Schuster · S. von Ende · S. Föll · R. Lammering

Received: 11 April 2012 / Revised: 16 November 2012 / Accepted: 13 December 2012

Abstract Accurate knowledge of the dispersion relations of guided waves in plates is important for the efficient use of Lamb wave-based damage-detection methods. In this paper, we introduce a method which aims at automatically extracting the dispersion curves from laser vibrometer measurement data in an easy and robust manner. This method works by Fourier transforming the measurement data into the wavenumber domain and then applying the matrix pencil method by Hua and Sarkar to extract the wavenumber-dependent frequencies. As an additional result, we are able to experimentally detect backward propagating waves in aluminium plates.

F. Schöpfer (✉) · T. Schuster
Institut für Mathematik, Carl von Ossietzky Universität, 26111 Oldenburg, Germany
e-mail: frank.schoepfer@uni-oldenburg.de

T. Schuster
e-mail: thomas.schuster@uni-oldenburg.de

F. Binder · A. Wöstehoff · S. von Ende · S. Föll · R. Lammering
Fakultät für Maschinenbau, Helmut-Schmidt-Universität, 22043 Hamburg, Germany
e-mail: binder@hsu-hh.de

A. Wöstehoff
e-mail: woestehoff@hsu-hh.de

S. von Ende
e-mail: Sven.vonEnde@rolls-royce.com

S. Föll
e-mail: foell@hsu-hh.de

R. Lammering
e-mail: rolf.lammering@hsu-hh.de

Keywords Dispersion curves · Guided waves · Matrix pencil method · Structural health monitoring · Backward propagating waves

1 Introduction

The study of the behaviour of guided waves in plates is of growing interest due to their potential use in non-destructive evaluation (NDE) and structural health monitoring (SHM), e.g. the comprehensive books of Giurgiutiu [5] and Rose [13]. Since guided wave propagation in thin plates is dispersive, i.e. the velocity of wave propagation depends on the frequency, many conventional damage-detection methods are no longer straightforward to apply, especially if they are based on time-of-flight measurements. Therefore, it is necessary to know the dispersion relations accurately. Based on the elastic wave equation, dispersion curves for elastic material can be computed numerically if the material parameters are known [1, 9, 10, 15]. Nevertheless, the elastic wave equation is an ideal model which approximates the complex behaviour of the actual material at hand. This is particularly true for composite structures which often are also modelled as elastic material. Hence, it is important to have a means to verify the validity of the model experimentally.

Time-of-flight based measurements of phase and group velocities suffer from difficulties in dealing with multiple modes and high velocities. Some methods using Fourier transforms in space and time and time–frequency analysis have been proposed to overcome these difficulties [2, 6, 12]. However, the determination of dispersion curves with these methods still often requires some graphical methods like extracting peaks of signals or ridges in two-dimensional surfaces, which is quite sensitive to noise.

Published online: 11 January 2013

In this paper, we introduce a method which aims at automatically extracting dispersion curves from laser vibrometer measurement data in an easy and robust manner. This method works by Fourier transforming the measurement data into the wavenumber domain and then applying the matrix pencil method by [8] to extract the wavenumber-dependent frequencies. Due to the high spatial and temporal resolution of the laser vibrometer and robustness of the matrix pencil method, we get very accurate results, which is confirmed by comparing the experimental results with the known theoretical values for aluminium plates. As an additional result, we are able to experimentally detect backward propagating waves in aluminium plates.

2 Dispersion relations via mode decomposition in the wavenumber domain

Let $U(\mathbf{x},t)$ be the out-of-plane component of the velocity vector of a wave travelling in the plate and let

$$\hat{U}(\mathbf{k},t) = \iint_{\mathbb{R}^2} U(\mathbf{x},t)\mathrm{e}^{-i\mathbf{k}^{\mathrm{T}}\mathbf{x}}\,\mathrm{d}\mathbf{x}$$

be its Fourier transform into the wavenumber domain, where

$$\mathbf{k}^{\mathrm{T}}\mathbf{x} = k_1x_1 + k_2x_2$$

is the standard scalar product of the vector $\mathbf{x} = (x_1,x_2)^{\mathrm{T}}$ of the space variables with the wave-vector $\mathbf{k} = (k_1,k_2)^{\mathrm{T}}$. After the initial excitation, there are supposed to be no external forces. Hence, we can decompose the signal $\hat{U}(\mathbf{k},t)$ into elementary wave modes, i.e. a sum of complex exponentials [15],

$$\hat{U}(\mathbf{k},t) = \sum_n a_n(\mathbf{k})\mathrm{e}^{2\pi i f_n(\mathbf{k})t},$$

where the sum is over all excited modes having a non-vanishing out-of-plane component, with wavenumber-dependent frequencies $f_n(\mathbf{k})$ and amplitudes $a_n(\mathbf{k})$. In theory, the sum may be infinite, but in practice, only a finite number μ of wave modes will make a major contribution to the signal and we can approximate the signal by a finite sum and some additive noise

$$\hat{U}(\mathbf{k},t) \approx \sum_{n=1}^{\mu} a_n(\mathbf{k})\mathrm{e}^{2\pi i f_n(\mathbf{k})t} + \text{noise}.$$

Now the dispersion relations are readily obtained by estimating μ and $f_n(\mathbf{k})$. This can be efficiently done with the help of the matrix pencil method by Hua et al. [8], which we will shortly describe in the next section.

Note that some noise in the above approximation is always unavoidable: on the one hand, we must approximate the continuous Fourier transform by a discrete version due to a finite number of samples. However, this discretization error will be small because of the high spatial resolution of the laser vibrometer. On the other hand, there will be a cutoff error due to a restricted measurement area $\Omega \subset \mathbb{R}^2$, i.e. we can only compute

$$\hat{U}(\mathbf{k},t) \approx \iint_{\Omega} U(\mathbf{x},t)\mathrm{e}^{-i\mathbf{k}^{\mathrm{T}}\mathbf{x}}\,\mathrm{d}\mathbf{x}.$$

The cutoff error can be made relatively small using wave packets with initially small support (of course after some time, such wave packets will dissolve due to dispersion). Nevertheless, the approximations are quite accurate and the matrix pencil method is robust to noise, which will be confirmed in our experiments.

We want to point out that the dispersion relations $f_n(\mathbf{k})$ may also be guessed by calculating for each wave-vector $\mathbf{k}$ the discrete Fourier transform of $\hat{U}(\mathbf{k},t)$ with respect to time. Fixing the direction of $\mathbf{k}$ and plotting the Fourier coefficients in a wavenumber–frequency-plane one can see the dispersion curves as ridges in the diagram (Fig. 1). Even if it is easy to identify those ridges visually, the extraction of the exact values from this two-dimensional surface would still be a hard task left to do, whereas using the method explained in this paper enables us to determine the exact values $f_n(\mathbf{k})$ automatically in an easy manner.

Furthermore, the matrix pencil method allows us to detect complex frequencies, which means that there is the possibility to measure damping from the same data without additional effort. This potential will be further exploited when we apply our method to examine anisotropic materials.

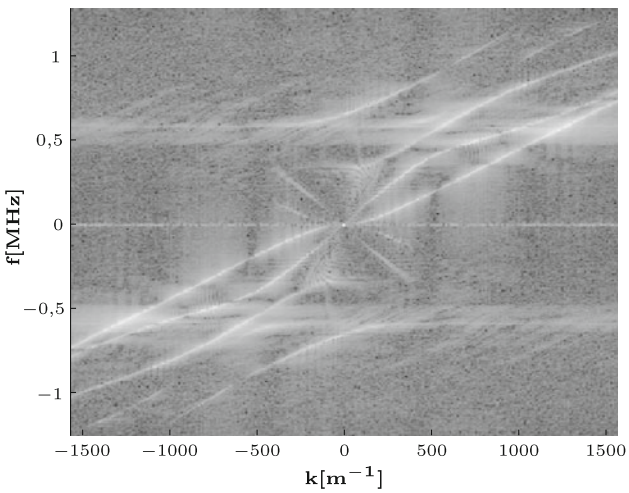

Fig. 1 Fourier coefficients of a measured wave in a wavenumber–frequency-plane

3 Estimating the number of modes and their wavenumber-dependent frequencies by the matrix pencil method

For each fixed wave-vector $\mathbf{k}$, we can form a data sequence $(u_l)_l$,

$$u_l := \hat{U}(\mathbf{k}, t_l) \approx \sum_{n=1}^{\mu} a_n(\mathbf{k}) z_n^{l-1}, \quad t_l := (l-1)/r_s, \quad l = 1, \ldots, \nu,$$

where r_s is the time-sample-rate, ν the number of samples which is supposed to be much larger than μ, and

$$z_n := \mathrm{e}^{2\pi i f_n(\mathbf{k})/r_s}, \quad n = 1, \ldots, \mu.$$

To estimate the number of modes and to get the dispersion relations $f_n(\mathbf{k})$, we follow [8] and use the matrix pencil method to estimate μ and extract the values z_n from the data sequence $(u_l)_l$. We shortly describe this method here and refer to [8, 14] for further information.

We form two $(\nu - \lambda) \times \lambda$ Hankel matrices $\mathbf{X_1}, \mathbf{X_2}$ from the data sequence $(u_l)_l$,

$$\mathbf{X_1} := \begin{pmatrix} u_1 & u_2 & \cdots & u_\lambda \\ u_2 & u_3 & \cdots & u_{\lambda+1} \\ \vdots & \vdots & & \vdots \\ u_{\nu-\lambda} & u_{\nu-\lambda+1} & \cdots & u_{\nu-1} \end{pmatrix}$$

and

$$\mathbf{X_2} := \begin{pmatrix} u_2 & u_3 & \cdots & u_{\lambda+1} \\ u_3 & u_4 & \cdots & u_{\lambda+2} \\ \vdots & \vdots & & \vdots \\ u_{\nu-\lambda+1} & u_{\nu-\lambda+2} & \cdots & u_\nu \end{pmatrix}.$$

The number λ is called the pencil parameter. If we choose λ such that

$$\mu \le \lambda \le \nu - \mu$$

then both matrices $\mathbf{X_1}, \mathbf{X_2}$ have rank μ and each z_n is a rank-reducing number for the matrix pencil

$$\mathbf{X_2} - z\mathbf{X_1}, \quad z \in \mathbb{C}. \tag{1}$$

Hence, the values z_n may be found as the μ generalized eigenvalues of the matrix pair $\mathbf{X_1}, \mathbf{X_2}$. However, since some noise is present and μ is a priori unknown, some precaution must be taken.

First, to combat noise a choice

$$\nu/3 \le \lambda \le \nu/2$$

for the pencil parameter λ was suggested in [8]. In our experiments, we obtained very good results for $\lambda = 5/12\ \nu$ (rounded), where the number of time samples was $\nu \ge 400$ and the expected number of modes $\mu \le 10$.

Second, singular-value decomposition (SVD) is used to estimate μ: let

$$\mathbf{X_1} = \mathbf{U\Sigma V}^*$$

be the reduced SVD of $\mathbf{X_1}$, where $\mathbf{U}$, $\mathbf{V}$ are matrices having orthonormal columns and $\mathbf{\Sigma} = \mathrm{diag}(\sigma_1, \sigma_2, \ldots)$ is a diagonal matrix containing the non-negative singular values of $\mathbf{X_1}$ in decreasing order. Then, μ is chosen to be the largest integer such that

$$\frac{\sigma_j}{\sigma_1} \ge \delta, \quad j = 1, \ldots, \mu,$$

where $0 < \delta < 1$ is a threshold, so that relatively small singular values are attributed to noise and will be discarded in the following way. Let $\tilde{\mathbf{\Sigma}} = \mathrm{diag}(\sigma_1, \ldots, \sigma_\mu)$ be the diagonal matrix containing only the first μ singular values of $\mathbf{X_1}$, and let $\tilde{\mathbf{U}}$, $\tilde{\mathbf{V}}$ be the matrices consisting of only the first μ columns of $\mathbf{U}$, $\mathbf{V}$, respectively. Multiplying the matrix pencil (1) with $\tilde{\mathbf{U}}^*$ from the left and with $\tilde{\mathbf{V}}$ from the right yields

$$\begin{aligned} \tilde{\mathbf{U}}^*\mathbf{X_2}\tilde{\mathbf{V}} - z\tilde{\mathbf{U}}^*\mathbf{X_1}\tilde{\mathbf{V}} &= \tilde{\mathbf{U}}^*\mathbf{X_2}\tilde{\mathbf{V}} - z\tilde{\mathbf{U}}^*\mathbf{U\Sigma V}^*\tilde{\mathbf{V}} \\ &= \tilde{\mathbf{U}}^*\mathbf{X_2}\tilde{\mathbf{V}} - z\tilde{\mathbf{\Sigma}}. \end{aligned}$$

Now we solve for the rank-reducing numbers of the modified pencil

$$\tilde{\mathbf{U}}^*\mathbf{X_2}\tilde{\mathbf{V}} - z\tilde{\mathbf{\Sigma}},$$

which in the noise-free case coincide with those of (1).

4 Experimental setup

The following experiment was carried out to measure the out-of-plane velocity at the top face of an elastic plate which is the main input to calculate the corresponding dispersion curves.

A circular piezoelectric ceramic with 16-mm diameter and 0.27-mm thickness is glued with Loctite 401 superglue to the surface of a 600 × 900 × 5 mm aluminum-plate. The out-of-plane velocity is measured along a line from the wave source to the boundary with a laser scanning vibrometer (Polytec PSV 400). The scanning path is equipped with a strip of reflector foil to improve the measured signal. As an additional improvement, the signal is averaged from 56 measurements.

The input signal—a rectangular burst with a frequency of 975 kHz—is generated by a Tektronix AFG 3021 single channel arbitrary function generator and is amplified with the help of a compact power amplifier (Develogic WBHV 2A600) to an amplitude of around 60 V_{pp}. In Fig. 2, the experimental setup is shown.

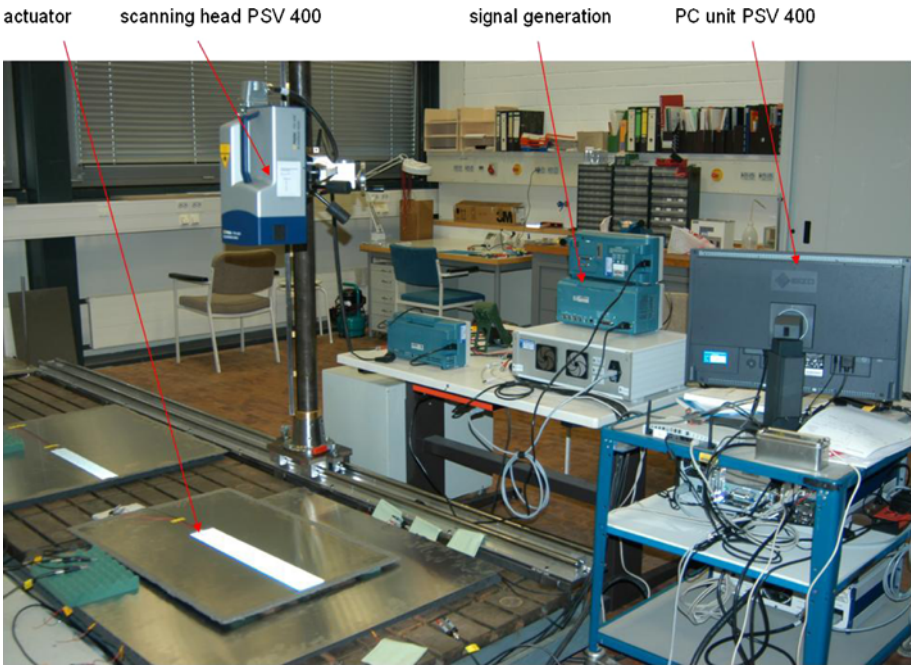

Fig. 2 Experimental setup (without function generator and amplifier)

5 From laser vibrometer measurement data to matrix pencil data

Since we examined an isotropic material, we measured all points in one line assuming a plane wave. The measurement area and, hence, the Fourier transform in space are only one-dimensional. We now can approach the problem from two different sides. Either we first calculate the discrete Fourier transform in space and then, use the matrix pencil algorithm to estimate the frequencies for each wavenumber, or we first calculate the discrete Fourier transform in time and afterwards use the matrix pencil algorithm to find wavenumbers associated with frequency. Although in theory, both approaches should yield the same result, in practice, one approach may perform better than the other, depending on the dataset. Since we found that they may discover complementary parts of the dispersion curves, we suggest to always perform both, compare Fig. 6. As both approaches work analogously, we will only describe in detail the first one.

The signal we used is a wave packet with support as small as possible. We chose it that way to reduce the cutoff error. A short pulse consists of a broader band in the wavenumber domain, so dispersion will cause the pulse to dissolve as the time passes. However, since we are interested in observing as many wavenumbers as possible, the cutoff error can hardly be avoided completely, hence, we employed windowed discrete Fourier transform to further improve the results.

The laser vibrometer data consisted of velocity values measured at $M = 488$ equidistant points in space and at $N = 400$ times, where the length of the scanning path was $L \approx 54.91$ cm and the duration of the measurement $T \approx 0.1562$ ms (Fig. 3).

The discrete wavenumbers obtained by the discrete Fourier transform with M samples in space are

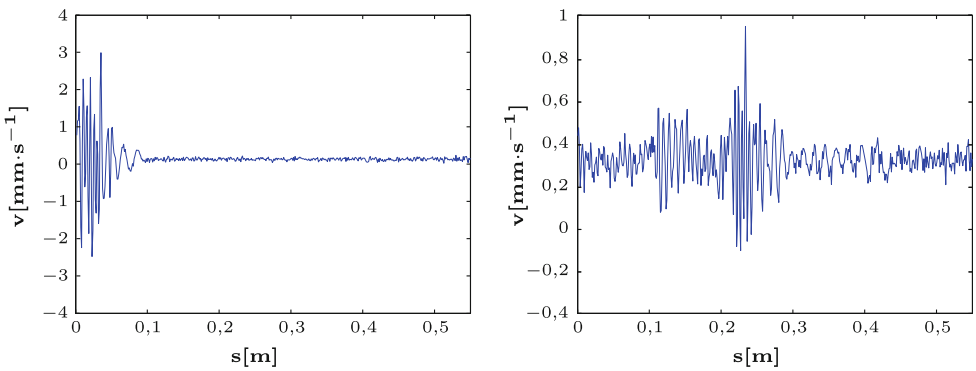

Fig. 3 The raw data at two different times. The out-of-plane velocity v versus the position s in the measurement area is plotted

$$\left\{-\frac{M}{2}+1,\ldots,0,\ldots,\frac{M}{2}\right\}\cdot\frac{2\pi}{L}.$$

Therefore, the highest measurable wavenumber is 2,784 m^{-1}.

For each time $t \in \{1\ldots N\}$, we have the measured, thus noisy sequence

$$(u_l^t)_l := (\tilde{u}_l^t)_l + \text{noise} \quad l \in \{1\ldots M\},$$

where $\tilde{u}_l^t$ would be the true noiseless data. From this sequence, we calculate the windowed discrete Fourier transform

$$\hat{u}_l^t = \sum_{n=0}^{M-1} w_n u_n^t \mathrm{e}^{-2\pi i\frac{nl}{M}}, \quad \text{for } l = 0\ldots M-1, \tag{2}$$

where w_l is a window-function to diminish the cutoff error. The sequence (2) is then used as input to the matrix pencil algorithm as described in Sect. 3.

Window functions usually feature Fourier transforms that have a narrow peak at 0, the main lobe, and several smaller side lobes. Window functions with smaller side-lobes have a wider main lobe and vice versa. Therefore, windowing can suppress the cutoff error with the drawback of a lesser accuracy regarding the position of the investigated signal on the frequency axis. We chose the Kaiser window as it possesses a parameter to control this trade-off between the main lobe's width and the side lobes' amplitudes. See [7] for further detail. The Kaiser window is defined as

$$w_n = \frac{I_0\left(\alpha\sqrt{1-\left(\frac{n-1-\frac{M}{2}}{M}\right)^2}\right)}{I_0(\alpha)}, \quad n = 1\ldots M,$$

where I_0 is the modified Bessel function of zeroth order. The parameter α controls the trade-off. The value $\alpha = 0$ corresponds to a rectangle window and as α increases, the window narrows, the main lobe widens and the side lobes' amplitudes decrease.

6 Results and detection of backward propagating waves

In all figures containing dispersion curves, red crosses and blue circles identify values determined from measurement data by the method described in this paper. Black solid lines represent the "true" dispersion curves based on the elastic model with literature values taken for the material parameters of aluminium. Since these curves have no explicit analytical description, they were computed numerically by use of the strip element method [4, 9, 15]. Dispersion diagrams are often plotted as phase velocity $c_\mathrm{p} = 2\pi\frac{f}{k}$ versus frequency f. In our situation, it is more convenient to plot frequency f versus wavenumber k. Of course, each of the diagrams can easily be obtained from the other. For a comparison, see Fig. 4, which also clarifies the names of the modes.

Figure 5 illustrates the influence of the parameters δ and α to the output of the algorithm. In the left column one can see that a lower threshold δ results in more points as potential candidates for dispersion curves, but also in more noise, whereas in the right column a higher window parameter α removes some of that noise. The diagrams are cropped at wavenumbers above $k = 1{,}760\,\mathrm{m}^{-1}$ due to more noise in that area.

Figure 6 compares the two approaches mentioned at the beginning of the previous section, namely using discrete Fourier transform in space and matrix pencil method in time or discrete Fourier transform in time and matrix pencil method in space. Apparently, both approaches show partly different sections of the dispersion curves and are, thus, complementing each other.

Let us elaborate a little further the way the dispersion diagrams are plotted, because actually they contain some more information which allowed us to experimentally detect backward propagating waves.

Calculating the (windowed) discrete Fourier transform in space, we obtain coefficients corresponding to both negative and positive wavenumbers. Since for each t, the sequence u_n^t is real, it holds that $\overline{\hat{u}_{M-l}^t} = \hat{u}_l^t$. This means that

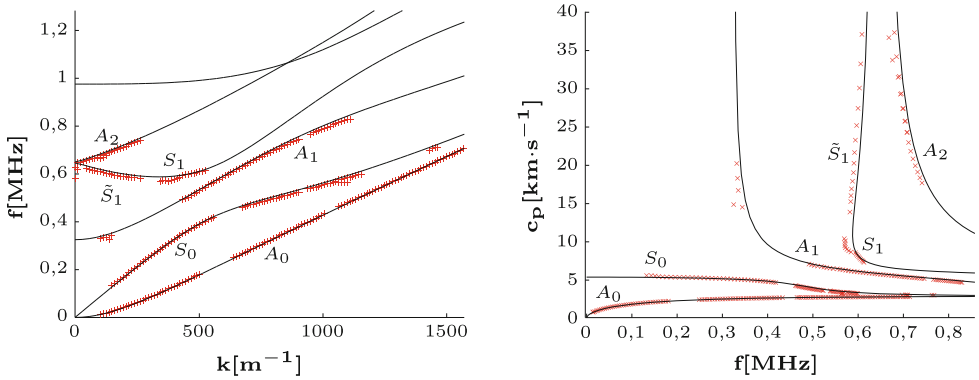

Fig. 4 A comparison between the $f-k$- and $c_\mathrm{p}-f$-diagrams

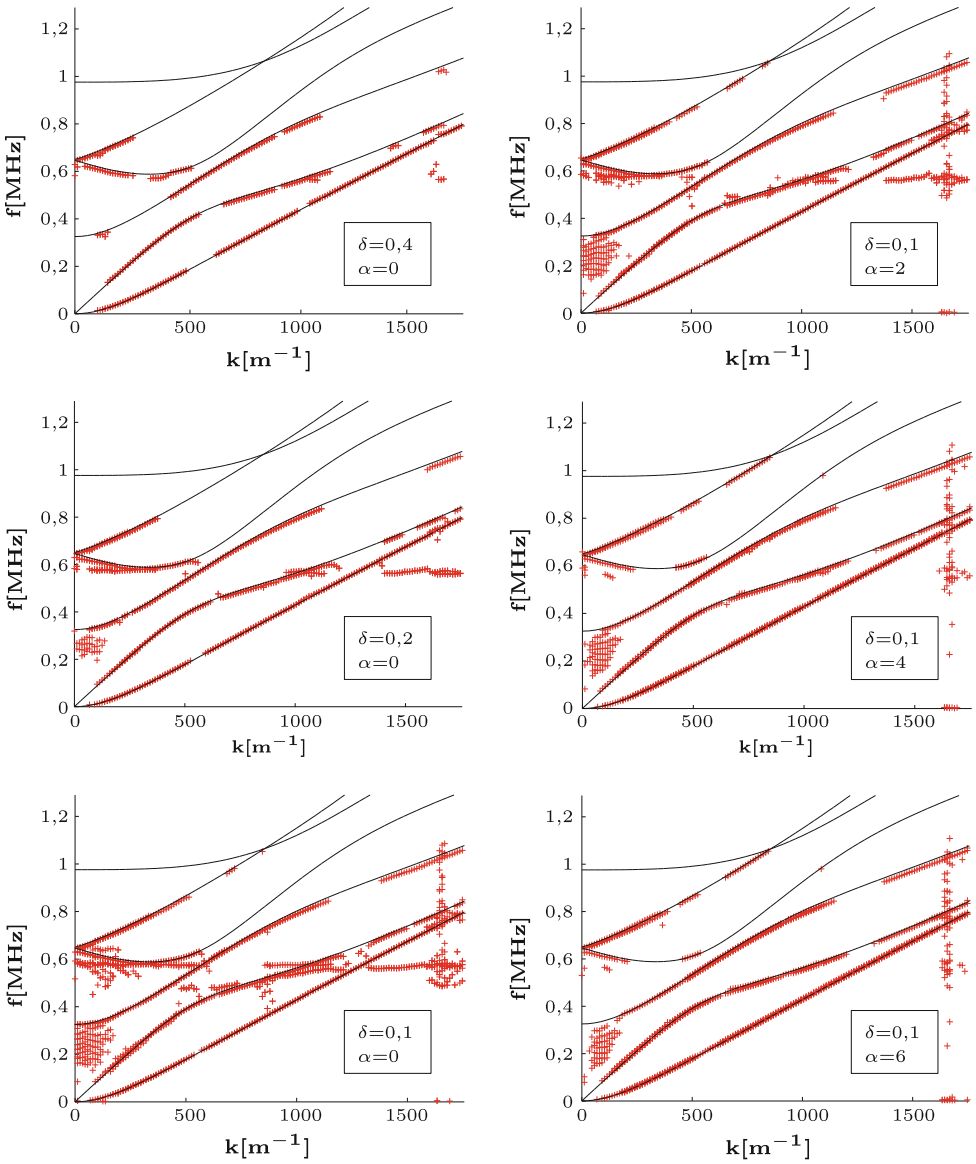

Fig. 5 A comparison of dispersion diagrams for different values of α and δ. *Left column* Influence of the threshold parameter δ of the matrix pencil method. It controls which part of the sum of exponentials approximating the Fourier-transformed signal is attributed to noise, where $\delta = 0$ means the whole sum is trusted. *Right column* Influence of the window parameter α. It controls the windowing function, where $\alpha = 0$ means rectangular windowing

we only have to take into account the positive wavenumbers, because for negative wavenumbers, the matrix pencil method will yield the same frequencies as for the corresponding positive ones, only with alternate sign. Nevertheless, we may get frequencies with negative signs, because the frequencies are extracted from complex exponentials and different signs contain information about the direction in which the waves are travelling. This information is partly lost in Figs. 4, 5 and 6, because we only plotted the absolute values of the frequencies determined with the matrix pencil method. To uphold this information, we plotted the frequencies with signs in Fig. 7.

Single-frequency waves are travelling with the phase velocity $c_\mathrm{p} = 2\pi\frac{f}{k}$ and small band wave groups are travelling with the group velocity $c_\mathrm{g} = 2\pi\frac{\mathrm{d}f}{\mathrm{d}k}$, [1]. Since we only plotted the positive wavenumbers, the sign of the phase velocity is determined by the sign of the frequency in Fig. 7, and the sign of the group velocity is determined by the slope of the respective dispersion curve. A positive sign means that the waves are travelling away from the source and a negative sign means that the waves are travelling towards the source. Hence, all red crosses in Fig. 7 indicate wave groups travelling away from the source. The blue circles belong to a wave group that was reflected at the boundary and is travelling towards the source.

Usually, the phase velocity and group velocity have the same sign. If they have different signs one speaks of backward propagating waves. The red crosses in the lower half of the diagram in Fig. 7 show that we have experimentally verified that this phenomenon actually occurs with guided waves in aluminium plates. Here, it occurs with a special symmetric wave mode, in Fig. 4, marked as

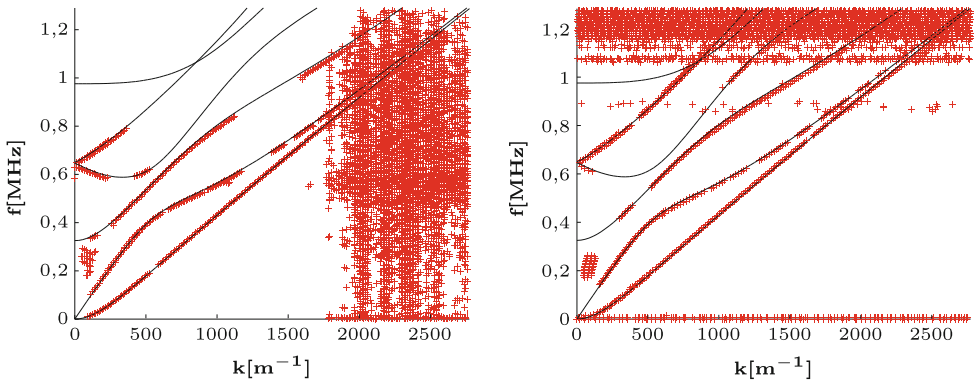

Fig. 6 In the *left diagram*, we applied the discrete Fourier transform in space and then, used the matrix pencil method in time, whereas in the *right diagram*, we applied the discrete Fourier transform in time and then, the matrix pencil method in space. Note that both approaches discover partly different sections of the modes, e.g. the fourth mode was better captured by the first approach, whereas the fifth mode for frequencies above 800 kHz was discovered only by the latter. The axes are chosen to show the theoretically maximum wavenumbers and frequencies. By this way, it is visible that the two approaches are sensitive to noise in different directions, an additional reason to perform both

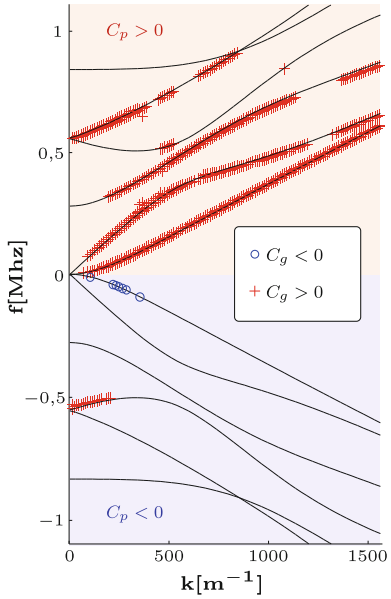

Fig. 7 All modes with the information on the sign of phase and group velocity. The phase velocity is positive in the *upper half* of the diagram and negative in the *lower half*. *Red crosses* indicate positive group velocity, *blue circles* negative. Hence, the *blue circles* belong to a wave group that was reflected at the boundary and is travelling towards the source. The *red crosses* in the *lower half* of the diagram indicate backward propagating waves

$\tilde{S}_1$, which has been described before in theoretical studies by [3]; see also [11]. It is excited in a small frequency band around 620 kHz together with the first appearance of the S_1 mode. Note that in many publications, such parts of the dispersion curves in $c_p - f$-diagrams are omitted.

Although by plotting only the absolute values of the frequencies in Figs. 4, 5 and 6, we loose the knowledge on the direction in which the waves are travelling, we still uphold the information on whether we deal with backward propagating waves.

7 Conclusions

We have demonstrated that applying the matrix pencil method to laser vibrometer measurement data is an easy and robust method to experimentally determine the dispersion curves of guided waves in plates. So far, accurate results have been obtained for aluminium plates where the experimentally determined values can be compared with known theoretical values. The method is not restricted to deal with isotropic material and the study of its effectiveness when dealing with anisotropic and laminated material is currently under investigation. Since our method also offers the possibility to extract complex frequencies and, thus, to measure damping without additional effort, this potential will also be exploited for composite structures where damping plays a decisive role.

Acknowledgments The work of F. Binder and T. Schuster is being supported by Deutsche Forschungsgemeinschaft (DFG) under Schu 1978/4-1.

References

1. Achenbach, J.D.: Wave Propagation in Elastic Solids. North-Holland, Amsterdam (1973)
2. Alleyne, D., Cawley, P.: A 2-dimensional Fourier transform method for the quantitative measurement of Lamb modes. In: Ultrasonics Symposium, 1990. Proceedings, IEEE 1990, vol. 2, pp. 1143–1146 (1990) doi:10.1109/ULTSYM.1990.171541
3. von Ende, S., Lammering, R.: Investigation on piezoelectrically induced Lamb wave generation and propagation. Smart Mater. Struct. **16**, 1802–1809 (2007)

4. Galan, J.M., Abascal, R.: Numerical simulation of Lamb wave scattering in semi-infinite plates. Int. J. Numer. Methods. Eng. **53**, 1145–1173 (2002). doi:10.1002/nme.331
5. Giurgiutiu, V.: Structural Health Monitoring with Piezoelectric Wafer Active Sensors. Academic Press, Amsterdam, Boston (2008)
6. Grondel, S., Assaad, J., Delebarre, C., Blanquet, P., Moulin, E.: The propagation of Lamb waves in multilayered plates: phase-velocity measurement. Meas. Sci. Technol. **10**, 348–353 (1999). doi:10.1088/0957-0233/10/5/002
7. Harris, F.J.: On the use of windows for harmonic analysis with the discrete Fourier transform. Proc. IEEE **66**, 51–83 (1978)
8. Hua, Y., Sarkar, T.: Matrix pencil method for estimating parameters of exponentially damped/undamped sinusoids in noise. IEEE Trans. Acoust. Speech Signal Process. **38**(5), 814–824 (1990)
9. Kausel, E.: Wave propagation in anisotropic layered media. Int. J. Numer. Methods. Eng. **23**, 1567–1578 (1986)
10. Lowe, M.J.S.: Matrix techniques for modeling ultrasonic waves in multilayered media. IEEE Trans. Ultrason. Ferroelectr. Freq. Control **42**(4), 525–542 (1995)
11. Prada, C., Balogun, O., Murray, T.W.: Laser-based ultrasonic generation and detection of zero-group velocity Lamb waves in thin plates. Appl. Phys. Lett. **87**. (2005) doi:10.1063/1.2128063
12. Prosser, W.H., Seale, M.D., Smith, B.T.: Time-frequency analysis of the dispersion of Lamb modes. J. Acoust. Soc. Am. **105**(5), 2669–2676 (1999)
13. Rose, J.: Ultrasonic Waves in Solid Media. Cambridge University Press, New York (1999)
14. Sarkar, T.K., Pereira, O.: Using the matrix pencil method to estimate the parameters of a sum of complex exponentials. IEEE Antennas Propag. Mag. **37**(1), 48–55 (1995)
15. Schöpfer, F., Binder, F., Wöstehoff, A., Schuster, T.: A mathematical analysis of the strip element method for the computation of dispersion curves of guided waves in anisotropic layered media. Math. Probl. Eng. **22**, 311–329 (2010)